#### Research Article

Zhiqiang Hu\* and Kaikun Wang

# Investigation into the thermal stability of a novel hot-work die steel 5CrNiMoVNb

https://doi.org/10.1515/htmp-2022-0031 received February 06, 2022; accepted March 25, 2022

Abstract: A novel hot-work die steel 5CrNiMoVNb is developed by optimizing the alloy composition of 5CrNiMoV steel. Thermal stability tests were carried out to compare the hardness evolution of the two steel types. The hardness reduction of 5CrNiMoVNb at 600 and 650°C was only 4.3HRC and 9.6HRC, while that of 5CrNiMoV steel at the same condition was as large as 6.5HRC and 17.5HRC, respectively, which suggests that the thermal stability of the 5CrNiMoVNb steel is more excellent. The thermal stability mechanism of 5CrNiMoVNb was studied based on microstructure analyses and thermodynamic calculations. This suggests that high tempering temperatures cause the coarsening of some carbides and suppress the recovery and recrystallization of the martensite matrix, which is the main reason for the slight decrease in the thermal stability. For the adding of the medium and strong carbide-forming elements, the carbides in 5CrNiMoVNb steel are mainly MC and M23C6 with low coarsening rate coefficient, and the content of these two carbides is almost constant below 670°C. The fine MC and M<sub>23</sub>C<sub>6</sub> carbides showed strong pinning and dragging effects on the dislocations and suppressed martensite recovery and recrystallization. Therefore, the novel hotwork die steel showed excellent tempering softening resistance and thermal stability than 5CrNiMoV steel.

**Keywords:** 5CrNiMoVNb steel, thermal stability, recovery and recrystallization, carbides, coarsening rate coefficient

Kaikun Wang: School of Material Science and Engineering, University of Science and Technology Beijing, Beijing 100083, China

#### 1 Introduction

At present, the commonly used hot-work die steels at home and abroad are H13, 3Cr2W8V, 5CrNiMoV, and some new hot-work die steels developed on their basis, which are all typical martensitic hot-work die steels. This type of hot-work die steel is characterized by high contents of medium or strong carbide-forming elements such as Cr, Mo, W, and V. These carbides, such as MC, M<sub>2</sub>C,  $M_7C_3$ , and  $M_{23}C_6$ , are controlled to precipitate and achieve the effect of precipitation hardening under reasonable heat treatment processes, thereby improving the thermal resistance, thermal stability, and wear resistance of the steels. Because most hot-work molds are generally exposed to high temperatures and pressures for prolonged periods, it is often prone to thermal fatigue crack, thermal wear, and partial fracture and thus may drastically reduce the actual service life of the die. The most influential parameters on thermal cracking are the surface temperature gradient of the die and the hardness and microstructure of the die material. In some studies, it has been observed that the thermal crack density and crack depth decrease with increasing surface hardness [1]. Thermal wear is a local loss of cohesion or the resulting material loss as a result of the cyclic action of contact stress and internal stress generated by external loads and thermal loads [2,3]. Research shows that die wear, fracture, and other failure modes of hot-work molds during service are ultimately due to the decrease in thermal softening and partial hardness accelerated by higher service temperatures [4-6]. Therefore, the softening resistance and thermal stability become the most important service properties for hot-work die steels.

Some investigations into the thermal stability of hotwork die steel suggest that it is dependent on the tempered microstructure and the precipitation strengthening phase [7–9]. The tempering temperature mainly influences the size and morphology of martensite and carbides [10]. When the mold is in service at a temperature between 500 and 700°C, the traditional martensitic die steel will exhibit recovery or recrystallization of the

<sup>\*</sup> Corresponding author: Zhiqiang Hu, School of Information Engineering, Suqian University, Suqian 223800, China; School of Material Science and Engineering, University of Science and Technology Beijing, Beijing 100083, China, e-mail: zqhu@squ.edu.cn

microstructure, coarsening of precipitates, and transformation of carbides, which lead to the softening and the reduction in hardness. Under the same tempering temperature and time, the smaller the maximum hardness decreases, the better the thermal stability of the steel [11]. The optimization of alloy composition and adjustment of the heat treatment process are the most commonly used methods to improve the softening resistance and thermal stability of hot-work die steels. Through optimization of the carbide-forming elements such as Cr, Mo, V, W, and Nb, increasing the content of secondary carbides with low coarsening rates and restraining the formation of large-size carbides, such as M<sub>23</sub>C<sub>6</sub> and M<sub>3</sub>C with high coarsening rates, are conducive to precipitation hardening [3,12–14]. In this article, a novel hot-work die steel 5CrNiMoVNb is developed based on the 5CrNiMoV steel. The thermal stability mechanism of the proposed hot-work die steel is analyzed based on the thermal hardness, microstructure evolution, and carbide precipitation.

# 2 Materials and experiments

#### 2.1 Materials

5CrNiMoV steel is a conventional martensitic hot-work die steel with excellent toughness and hardenability, which is widely used to produce various large or medium forging hammer dies and trimming dies. However, owing to its low temper resistance and thermal stability, 5CrNiMoV steel shows that a short thermal fatigue life and failure fracture easily occurs when it is used under relatively harsh working conditions. Therefore, a new hot-work die steel 5CrNiMoVNb is developed by optimizing the alloy

composition. The chemical compositions of 5CrNiMoV and 5CrNiMoVNb steels are shown in Table 1. The 5CrNiMoV steel for the experiment is taken from a large 12-ton hot-work die, and the heat treatment process is oil quenching at 870°C and tempering at 550°C for 2h. The 5CrNiMoVNb steel is a new type of hot-work die steel developed based on the 5CrNiMoV steel by optimizing the alloy elements through thermodynamic calculations. A 25 kg ingot is obtained by vacuum casting, and hot forging is performed with an eight forging ratio after heating at 1,180°C for 8 h. Afterward, forging is annealed at 850°C, and the next heat treatment process is quenching at 940°C and tempering at 600°C for 2h. The mechanical properties of the two test steels in a heattreated state are shown in Table 2. The values of elongation after fracture of 5CrNiMoV and 5CrNiMoVNb are not much different, being 10.13 and 11.40%, respectively. However, the tensile strength, hardness, and impact toughness of the 5CrNiMoVNb steel are increased by 29.4, 32.2, and 33.4%, respectively, compared with those of the 5CrNiMoV steel. This shows that the comprehensive mechanical properties of the 5CrNiMoVNb steel at room temperature are better than those of the 5CrNiMoV steel.

## 2.2 Experimental procedures

The initial dimensions of the specimens for the thermal stability tests were  $10~\text{mm} \times 10~\text{mm} \times 5~\text{mm}$ . To compare the thermal stability of the 5CrNiMoVNb steel with that of the 5CrNiMoV steel, a similar hardness of 42HRC was obtained for the two steels through other two different heat treatment processes, as shown in Table 2. The thermal stability tests were carried out in a box-type resistance furnace. The pretreated specimens were respectively tempered for different times at 600 and 650°C. The hardness of the

Table 1: Chemical composition of 5CrNiMoV and 5CrNiMoVNb steel

Steel	С	Si	Cr	Mn	Cu	Ni	Мо	V	Nb	Fe
5CrNiMoV	0.54	0.25	0.96	0.72	0.12	1.58	0.36	0.074	_	Bal.
5CrNiMoVNb	0.55	0.24	0.97	0.70	0.12	1.55	1.80	0.80	0.02	Bal.

Table 2: Mechanical properties of 5CrNiMoV and 5CrNiMoVNb steel

Steel	Hardness (HRC)	Impact energy (J)	Tensile strength (MPa)	Elongation (%)
5CrNiMoV	36.2	15.5	1,360	10.16
5CrNiMoVNb	48.3	20.5	1,761	11.40

specimens was measured by an MH-3-type microhardness tester. The microstructures of 5CrNiMoVNb and 5CrNiMoV steel specimens were examined by scanning electron microscopy (SEM; Zeiss Auriga, operated at 20 kV), transmission electron microscopy (TEM; TecnaiF30, operated at 200 kV), and energy-dispersive spectroscopy (EDS). To acquire the SEM specimens, the samples were first ground and polished through multiple passes to remove surface scratches and then corroded by a 4% nitric acid alcohol solution for about 15 s. The TEM specimens were first ground to a thickness of about 50 µm and then round specimens with a diameter of 3 mm were obtained by a punch. Finally, the specimens were thinned by a twin-jet electropolishing device, and the electrolyte was 5% perchloric acid with methanol. The voltage for thinning was about 12 V, and the electrolyte temperature was maintained at -20°C (Table 3).

## 3 Results and discussions

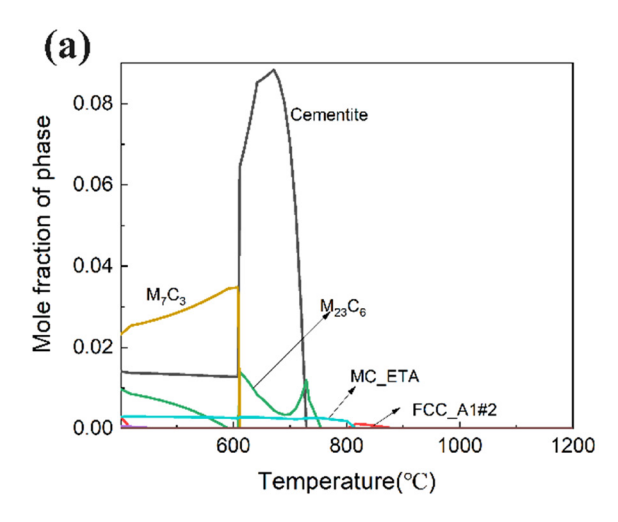
### 3.1 Analysis of equilibrium phase

As shown in Figure 1, thermodynamic calculations on a multiphase and multicomponent balance were used to analyze the precipitates' content and their transformation with temperature for 5CrNiMoV and 5CrNiMoVNb steels. For the 5CrNiMoV steel, the main precipitates include  $M_7C_3$ , cementite,  $M_{23}C_6$ , and  $MC_ETA$  when the temperature is below 610°C. The highest mole fraction of the precipitates is carbide  $M_7C_3$ , which is composed of C, Fe, Cr, Mn, Mo, and V. As the temperature increases, the mole fraction of C in  $M_7C_3$  is almost constant, but the

mole fraction of Fe increases a lot by replacing Mn and Cr. When the temperature is higher than 610°C, the carbide M<sub>7</sub>C<sub>3</sub> disappears and the main precipitate transforms into cementite with lower hardness and higher coarsening rate. For the 5CrNiMoVNb steel, when the temperature is lower than 670°C, the main precipitates are  $MC_ETA$ ,  $M_{23}C_6$ , and  $M_7C_3$ , and their mole fractions remain almost unchanged. Compared with the 5CrNiMoV steel, the precipitates in the 5CrNiMoVNb steel are significantly increased, especially MC\_ETA carbide. As is known that MC has a low coarsening rate and usually exists in the form of fine particles, which contributes to a strong precipitation strengthening effect. The increase of Mo and V elements and the addition of a small amount of Nb element greatly increase the content of MC\_ETA, and the content is relatively stable. Thus, the 5CrNiMoVNb steel is likely to have more outstanding toughness and excellent hightemperature thermal stability (Figure 2).

#### 3.2 Hardness evolution

As shown in Figure 3, the hardness of 5CrNiMoV and 5CrNiMoVNb steels depends on the tempering time and temperature. As the tempering time increases, the hardness values of the two steels first decrease rapidly and then tend to remain constant. The initial hardness values of the 5CrNiMoV and 5CrNiMoVNb steels are 42.4HRC and 41.9HRC, respectively. After tempering at 600°C for 24 h, the hardness values of the two steels are reduced to 35.9HRC and 37.6HRC, respectively, and the hardness decreases were 6.5HRC and 4.3HRC, respectively. After being tempered at 650°C for 24 h, the hardness values of



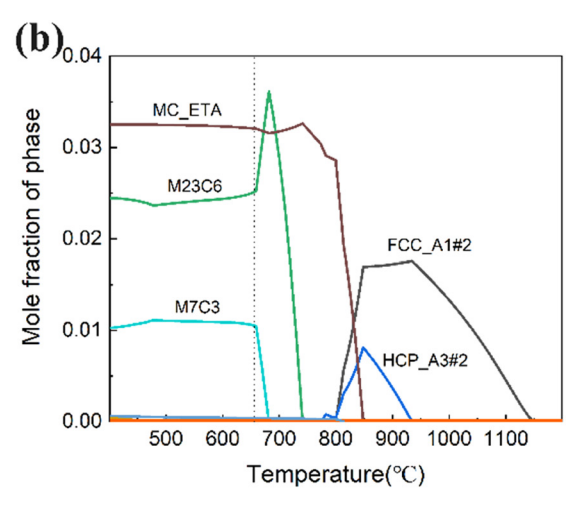


Figure 1: The balanced precipitates of the two steels: (a) 5CrNiMoV and (b) 5CrNiMoVNb.

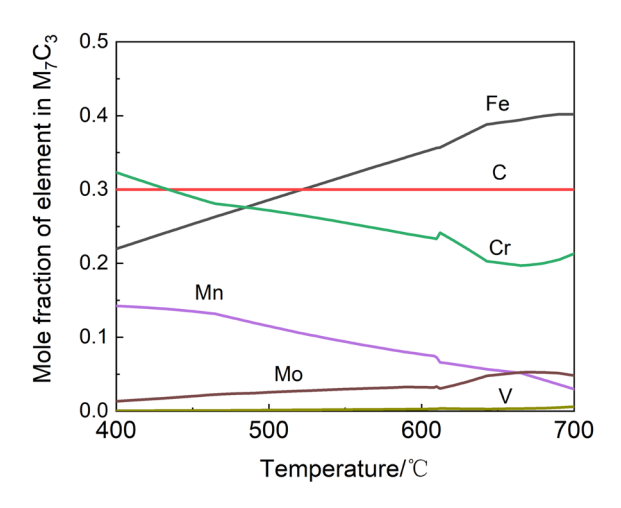


Figure 2: The element mole fraction of M7C3 in 5CrNiMoV steel.

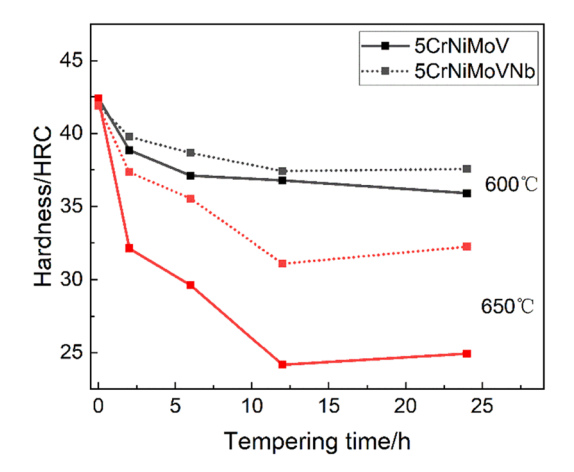


Figure 3: The dependence of hardness in 5CrNiMoV and 5CrNiMoVNb steels on tempering time and temperature.

Table 3: The heat treatment process

Steel	The heat treatment process	Hardness (HRC)
5CrNiMoV	880°C quenching, 560°C tempering for 2 h	42.4
5CrNiMoVNb	860°C quenching, 620°C tempering for 2 h	41.9

5CrNiMoV and 5CrNiMoVNb steels decreased to 24.9HRC and 32.3HRC and the hardness decreases were 17.5HRC and 9.6HRC, respectively. Generally, the hardness reduction of the 5CrNiMoVNb steel at 600 and 650°C is 35 and 45% lower than that of the 5CrNiMoV steel, respectively. This shows that the thermal stability and tempering softening resistance of the 5CrNiMoVNb steel are significantly better than those of the 5CrNiMoV steel. Besides, as shown in Table 4, compared with other commonly used hot-work

Table 4: The hardness value of several hot-work die steels tempered at 650°C for 24 h

Steel	Hardness (HRC)	Hardness decrease (HRC)
5CrNiMoV	24.9	17.5
5CrNiMoVNb	32.3	9.6
DM	32.6	14.6
H21	30.4	16.3
H13	25.6	20.9

die steels, such as DM, H21, and H13 steel, the hardness decrease of the 5CrNiMoVNb steel at 650°C for 24 h is at a low level, which suggests that the thermal stability of the 5CrNiMoVNb steel is more excellent.

#### 3.3 Microstructure evolution

The hardness values and the thermal stability usually depend on the tempering microstructure. As shown in Figure 4, the initial microstructure of the two steels prior to the thermal stability test is made up of lath martensite and fine secondary carbides, most of which are evenly dispersed on martensite. Besides the low alloy content of the two steels, there are nearly no large primary carbides. Due to the relatively high tempering temperature for the 5CrNiMoVNb steel during the pretreatment, the initial microstructure is slightly coarsened with recovery characteristics.

The tempered microstructure of the two steels at 600°C for 2 and 24 h is shown in Figure 5. At the beginning of the thermal stability test, there was no obvious change in the tempered microstructure of both two steels. After being tempered for 24 h, the carbides are slightly coarsened, and the martensite matrix is recovered in both steel alloys. It is shown that the tempered martensitic lath of the 5CrNiMoV steel is abnormally coarsened and relatively large compared with that of the 5CrNiMoVNb steel. The tempered microstructure of the two steels at 650°C for 2 and 24 h is shown in Figure 6. After tempering for 2 h, the microstructure of both steels is recovered and the martensite lath occurs to disappear. Fine carbides begin to accumulate and grow, and large particles of carbides appear. As the tempering time increases to 24 h, the microstructures of both steels are coarsened and recrystallized, and the martensite lath almost disappears. Some carbides are abnormally coarsened, and most carbides are distributed at the grain boundaries rather than on the matrix. Generally, there are two main factors affecting the thermal stability of the steels. One is the evolution of

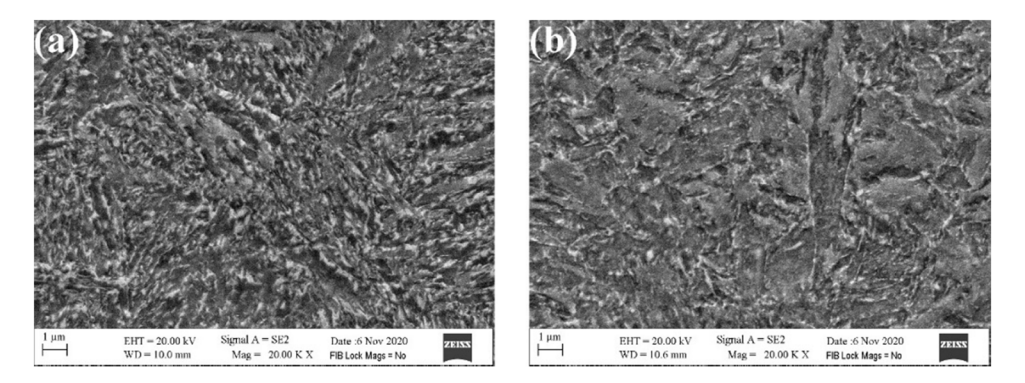


Figure 4: The initial microstructure of the two steels by SEM: (a) 5CrNiMoV and (b) 5CrNiMoVNb.

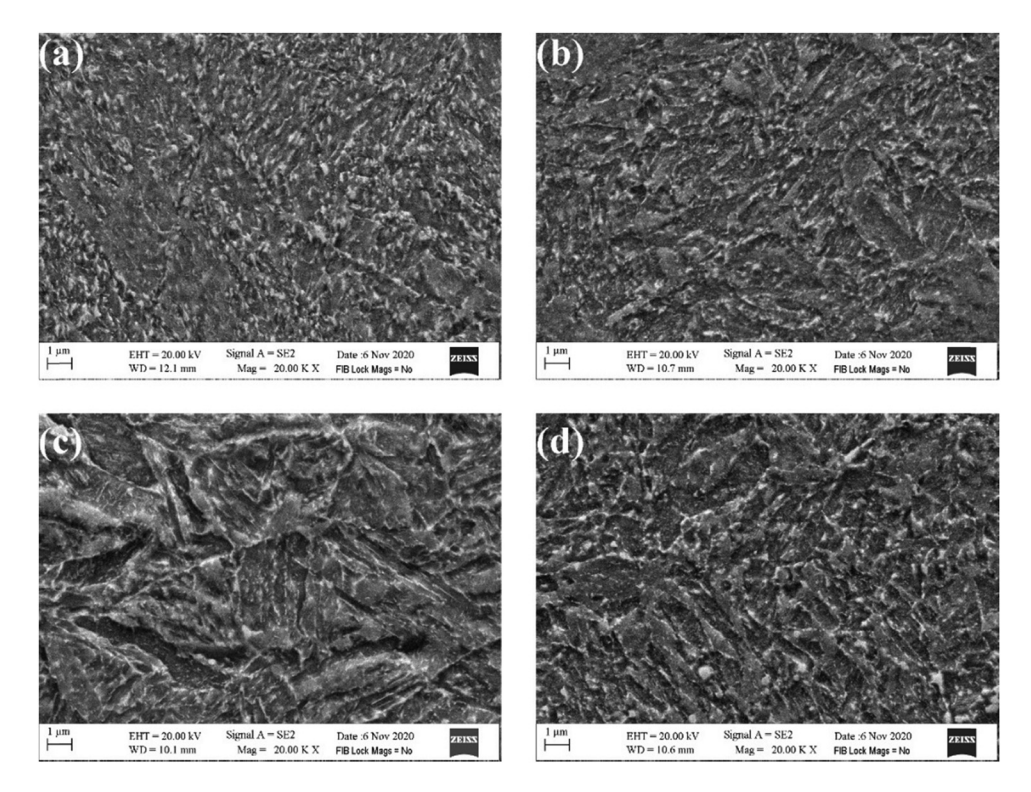


Figure 5: The tempered microstructure of the two steels by SEM at 600°C for different tempering times: (a) 2 h-5CrNiMoV, (b) 2 h-5CrNiMoVNb, (c) 24 h-5CrNiMoV, and (d) 24 h-5CrNiMoVNb.

the second phase caused by hot activation energy and element diffusion, and the other is the recovery and recrystallization of the microstructure due to the release of distortion energy. By comparing the microstructures between 5CrNiMoV and 5CrNiMoVNb steels, it is found that the new hot-work die steel 5CrNiMoVNb has a low carbide coarsening rate and low martensite recovery and recrystallization at the same thermal stability test conditions. Therefore, the thermal stability and the temper softening resistance of the 5CrNiMoVNb steel are significantly better than those of the 5CrNiMoV steel.

To further analyze the thermal stability mechanism of the novel hot-work die steel 5CrNiMoVNb, the evolution of the microstructure and the types, morphology, and distribution of carbides of the two steels under different thermal stability test conditions are analyzed and compared. The initial microstructure of the two steels by TEM is shown in Figure 7. As shown in Figure 7a, the carbides in the 5CrNiMoV steel are mostly long strips with a width of 30–50 nm. A selected-area diffraction pattern of a long-strip carbide (particle A) shows that the measured angle between the crystal planes (001)

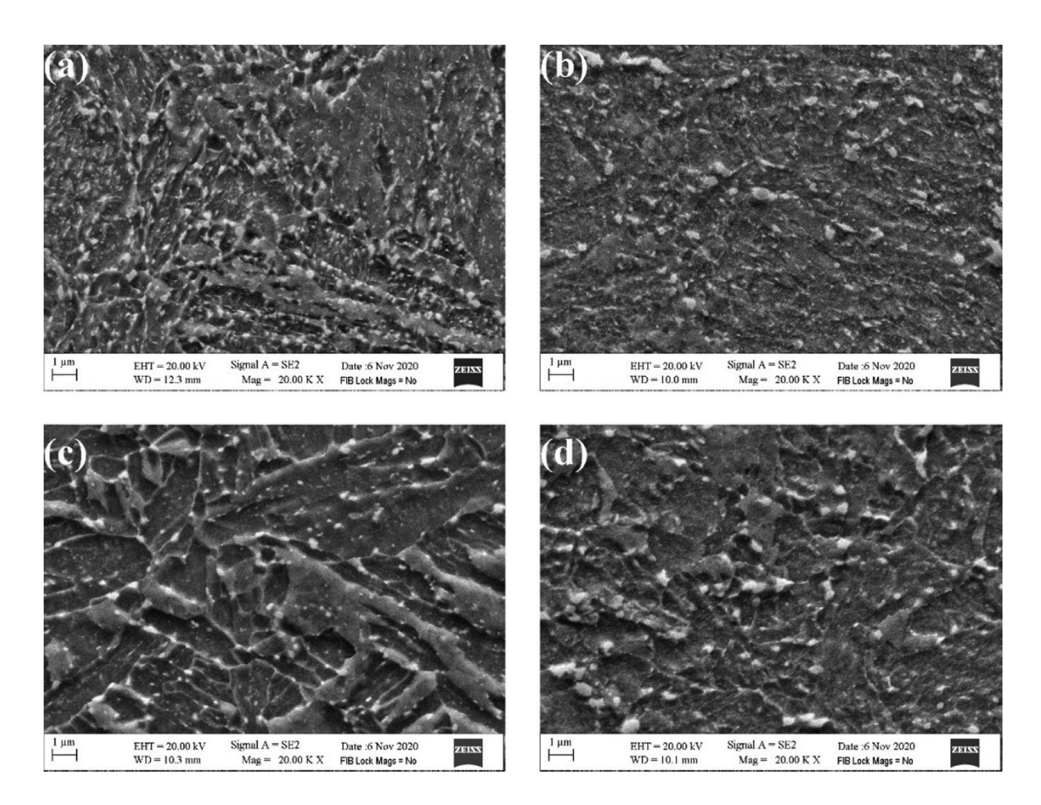


Figure 6: The tempered microstructure of the two steels by SEM at 650°C for different tempering time: (a) 2 h-5CrNiMoV, (b) 2 h-5CrNiMoVNb, (c) 24 h-5CrNiMoV, and (d) 24 h-5CrNiMoVNb.

and (-110) is 89.53°, which is close to the theoretically calculated value of 90°. After acquiring other crystal face indices through the vector algorithm, the long-strip carbide is calibrated as the orthorhombic M<sub>7</sub>C<sub>3</sub> carbide and the crystal zone axis is (110). The EDS result shows that the long-strip carbide is enriched with Fe, Cr, Mn, and Cu. Compared with M<sub>7</sub>C<sub>3</sub> carbides with a close-packed hexagonal structure, the orthorhombic M<sub>7</sub>C<sub>3</sub> carbides have more excellent thermal stability [15], which shows a positive effect on the thermal stability of the 5CrNiMoV steel. As shown in Figure 7b, most of the carbides in the 5CrNi-MoVNb steel are fine and granular. A relatively large carbide (particle B) is analyzed through diffraction (Figure 7d) and energy (Figure 7f) spectra. It suggests that particle B is a face-centered cubic M<sub>23</sub>C<sub>6</sub>-type carbide, which is enriched with the elements of Fe, Cr, and Mo. Combining the results of thermodynamic calculations and the analyses of energy spectra of elements, these fine carbides are identified as MC-type carbides. A mass of dislocations is found to be distributed at the boundaries of the martensite slabs, and a few carbides are found around the dislocation cells. This suggests that the movement of dislocations is easily inhibited by carbides and lath boundaries [16,17], resulting in the formation of dislocation cells and high-dislocation-density regions [18,19].

The carbides in the 5CrNiMoVNb steel with an average size of 20 nm are distributed evenly throughout the martensite matrix, which has a stronger pinning effect on dislocations. Therefore, compared with the 5CrNiMoV steel, the 5CrNiMoVNb steel has stronger resistance to temper softening and better thermal stability.

Figure 8 shows the tempered microstructures of the two steels by TEM at 600°C for different tempering times. Comparing the martensite and carbides of the 5CrNiMoV steel tempered for 2 and 24 h, the martensite is recovered to a certain extent and clear martensite lath boundaries and a small amount of entangled dislocations can still be observed. Compared with the carbides in the 5CrNiMoV steel tempered for 2h, the carbides are obviously coarsened, and a small amount of large-particle carbides appears after being tempered for 24 h. For the 5CrNi-MoVNb steel, with the extension of the tempering time, the martensite is slightly recovered and the carbides are hardly coarsening. A number of dislocation cells still remain on the martensite matrix. By analyzing the diffraction and energy spectra, particle A in Figure 8d is suggested to be a hexagonal close-packed MC-type carbide with the elements of Mo and V, and the carbides hardly coarsen during the tempering. Research shows that the carbide MC is prone to segregation of Mo atoms

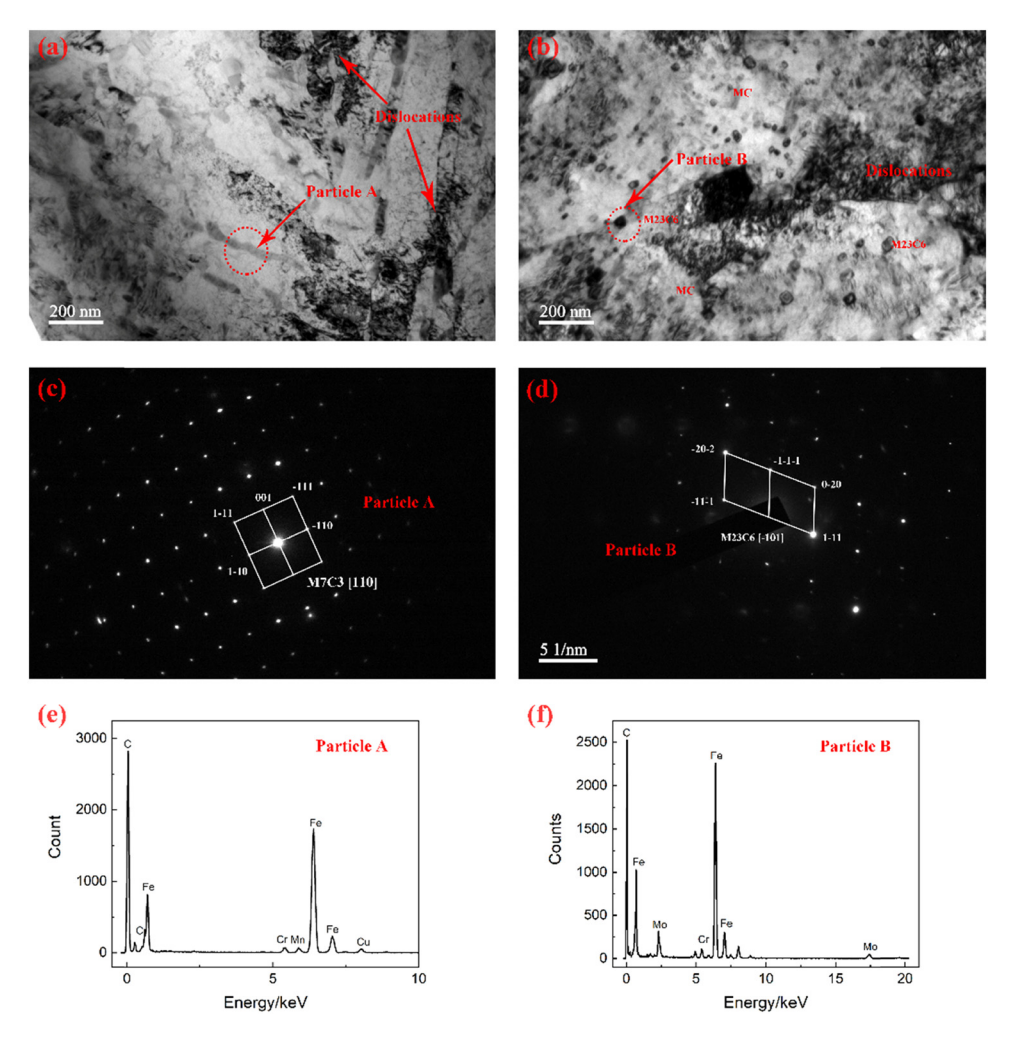


Figure 7: The initial microstructure of the two steels by TEM: (a) 5CrNiMoV, (b) 5CrNiMoVNb, (c) diffraction of particle A, (d) diffraction of particle B, (e) energy spectra of particle B.

to form a Mo-rich layer, which hinders the diffusion of other atoms such as V and Nb into the MC carbide. The Mo-rich layer formed by segregation reduces the coarsening rate by reducing the diffusion rate of C and alloying elements in the MC carbide [20,21]. Besides, element Mo reduces the formation energy of MC carbide and the interface energy between the MC carbide and ferrite [22,23]. Therefore, the (Mo,V)C carbides with a higher degree of coherence with the matrix in the 5CrNiMoVNb steel are fine particles and dispersed on the martensite matrix, which improves the strong plasticity, thermal hardness, and thermal stability of the 5CrNiMoVNb steel to a certain extent.

Figure 9 shows the tempered microstructures of the two steels by TEM at 650°C for different tempering times. The martensite for the 5CrNiMoV steel obviously recovers and recrystallizes after being tempered at 650 for 2 h. Only a small amount of carbides remains in the matrix,

and most of the carbides are coarsened and gathered at the grain boundaries. According to the analysis of the diffraction and the energy spectra for most carbides, the carbide with the highest content is orthorhombic M<sub>3</sub>C, which has lower hardness and is easy to coarsen. After being tempered at 650 for 2 h, most carbides dissolve into the matrix and a few large-sized carbides are distributed on the grain boundaries of the recrystallized microstructure. Different from the 5CrNiMoV steel, although the martensite is also recovered and recrystallized for the 5CrNiMoVNb steel after being tempered at 650 for 2h, a large number of MC carbides are still dispersed in the matrix, and M<sub>23</sub>C<sub>6</sub> carbides have not been significantly coarsened. Besides, there are still sparse dislocation lines distributed in the martensite lath, which reflects the pinning and dragging effects of fine carbides on the dislocations. However, as the tempering time increases, a large amount of little carbides dissolve into the matrix and the

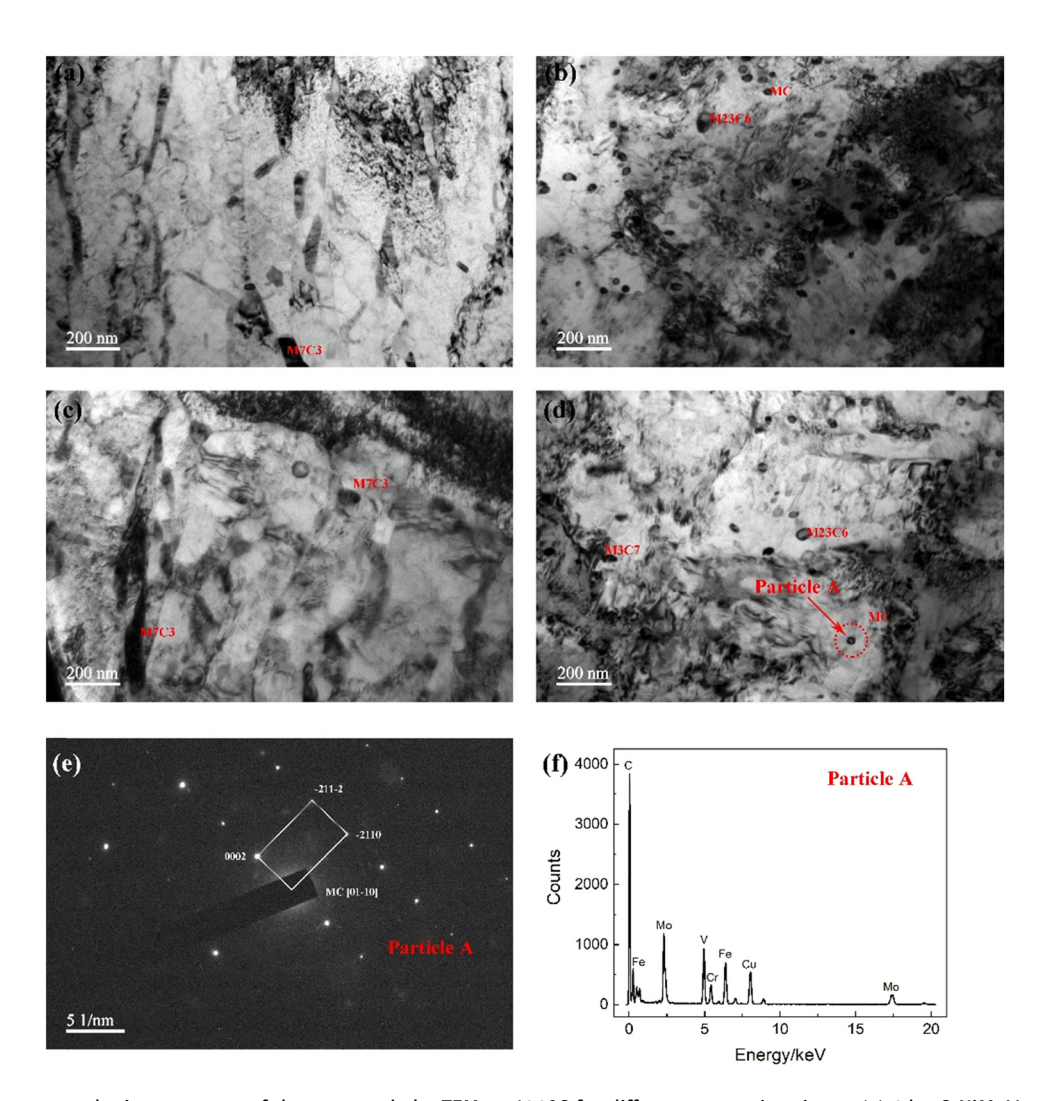


Figure 8: The tempered microstructure of the two steels by TEM at 600°C for different tempering times: (a) 2 h-5CrNiMoV, (b) 2 h-5CrNiMoVNb, (c) 24 h-5CrNiMoV, (d) 24 h-5CrNiMoVNb, (e) diffraction of particle A, and (f) energy spectra of particle A.

carbides at the grain boundaries begin to coarsen, which is due to the fact that the fine carbides have a high chemical potential. At the same time, depletion of alloying elements and carbon elements easily occurs inside the grains, which causes the transformation of high coherent carbides to low-coherent and noncoherent carbides. Therefore, the thermal stability and thermal hardness of the 5CrNiMoVNb steel decrease significantly at 650°C, but these are still higher than those of the 5CrNiMoV steel.

## 3.4 Coarsening behavior of carbides

Table 5 shows the mass fraction of main carbides in the 5CrNiMoV and 5CrNiMoVNb steel at 600 and 650°C. Based on the TCFE7 and MOBFE3 database of Thermo-Calc software, the application property calculation module

is used to calculate the coarsening rate coefficients of the main carbides in the temperature range of 500-725°C, which is shown in Figure 10. For the 5CrNiMoV steel, the main precipitation strengthening phases are 0.281% alloy cementite and 2.720% M<sub>7</sub>C<sub>3</sub> carbide at the temperature of 600°C, where the coarsening rate coefficient of M<sub>7</sub>C<sub>3</sub> is only  $0.0247 \times 10^{-29} \,\mathrm{m}^3 \cdot \mathrm{s}^{-1}$ . When the temperature increases to 650°C, M<sub>7</sub>C<sub>3</sub> disappears and the main precipitation strengthening phases becomes 7.017% alloy cementite and 0.667% M<sub>7</sub>C<sub>3</sub> carbide. At this time, the carbide coarsening rate coefficient of the alloy cementite has increased by two orders of magnitude. The coherent relationship between the large-particle carbide and the matrix is basically lost, and the precipitation strengthening effect is severely weakened. Therefore, the 5CrNiMoV steel shows poor thermal hardness and thermal stability at 650°C. For the 5CrNiMoVNb steel, the precipitation

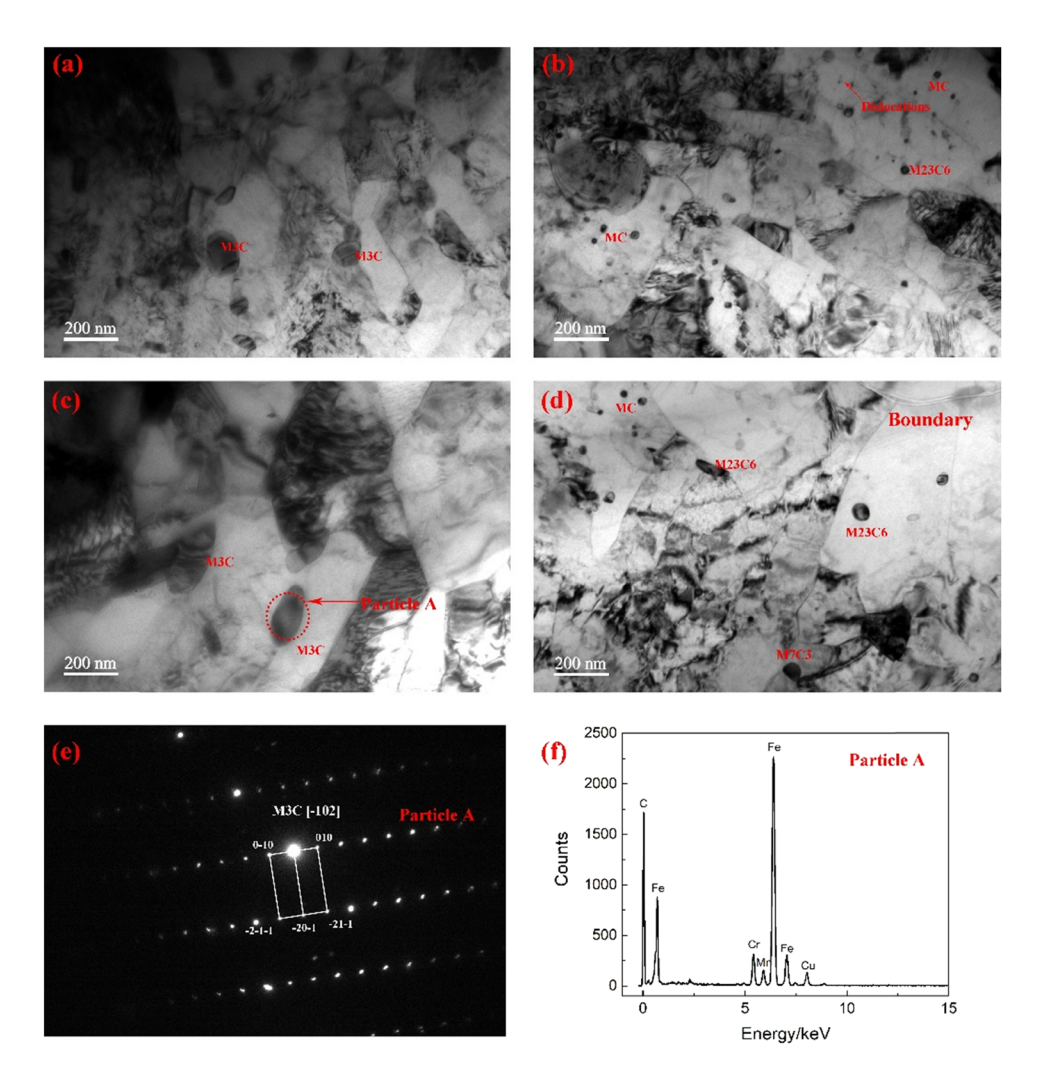


Figure 9: The tempered microstructure of the two steels by TEM at 650°C for different tempering times: (a) 2 h-5CrNiMoV, (b) 2 h-5CrNiMoVNb, (c) 24 h-5CrNiMoV, (d) 24 h-5CrNiMoVNb, (e) diffraction of particle A, and (f) energy spectra of particle A.

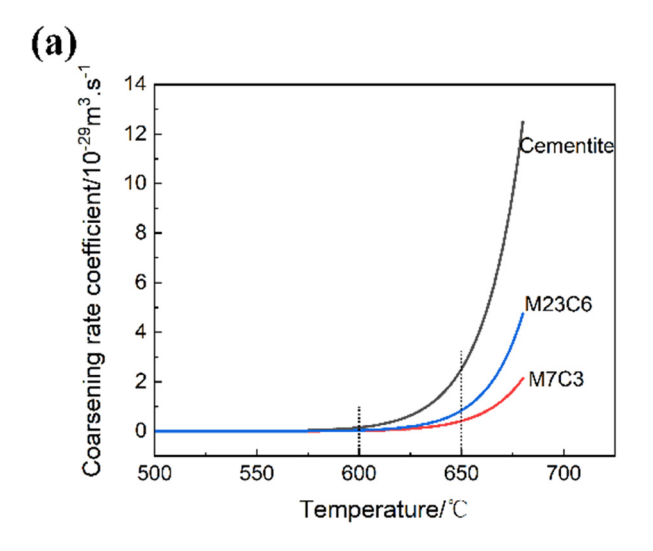
**Table 5:** Mass fraction of carbides in the two steels at different equilibrium temperatures (%)

M <sub>7</sub> C <sub>3</sub>	M <sub>23</sub> C <sub>6</sub>	M <sub>3</sub> C	MC
2.720	0	0.281	0
0	0.669	7.017	0
0.848	2.187	0	2.473
0.825	2.232	0	2.457
	2.720 0 0.848	2.720 0 0 0.669 0.848 2.187	2.720 0 0.281 0 0.669 7.017 0.848 2.187 0

strengthening phases are mainly MC,  $M_{23}C_6$ , and  $M_7C_3$  below 670°C, and the content remains almost unchanged as the temperature decreases. The coarsening rate coefficient of MC,  $M_{23}C_6$ , and  $M_7C_3$  at 600°C are  $9.27 \times 10^{-35}$ ,  $0.033 \times 10^{-29}$ , and  $0.024 \times 10^{-29}$  m<sup>3</sup>·s<sup>-1</sup>, respectively, which

suggests that the precipitated phase basically does not coarsen during the process of the long-term thermal stability test at 600°C. When the temperature rises to 650°C, the coarsening rate coefficients of MC,  $M_{23}C_6$ , and  $M_7C_3$  increase to  $3.66\times10^{-33},\ 0.684\times10^{-29},\ and\ 0.409\times10^{-29}\ m^3\cdot s^{-1},$  respectively. Although the coarsening rate coefficients of the three carbides have increased to a certain extent, the MC carbide with the highest content still maintains a very low coarsening rate. Therefore, as the temperature increases, the thermal stability of the 5CrNiMoVNb steel is slightly reduced, but it still has good thermal stability compared with the 5CrNiMoV steel.

Based on the TEM carbide analysis of the 5CrNiMoVNb steel during the thermal stability test, ImagePro software was used to calculate the carbide sizes of MC and  $M_{23}C_6$  with higher contents, as shown in Figure 11. After tempering at 600 and 650°C for 24 h, the size of the MC carbide



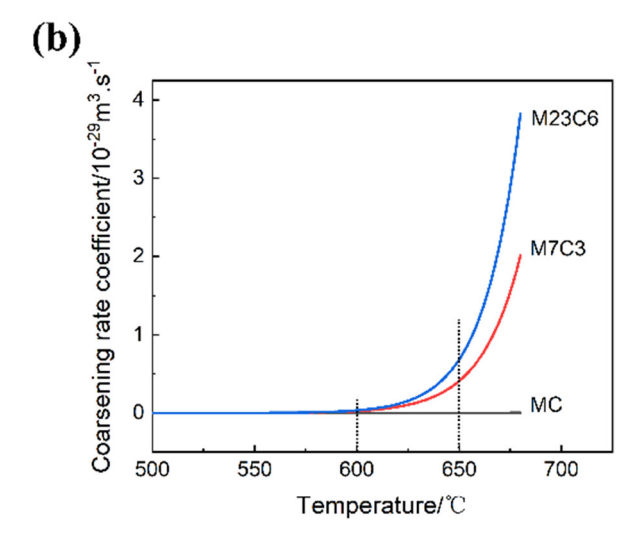


Figure 10: The influence of temperature on carbide coarsening rate coefficient.

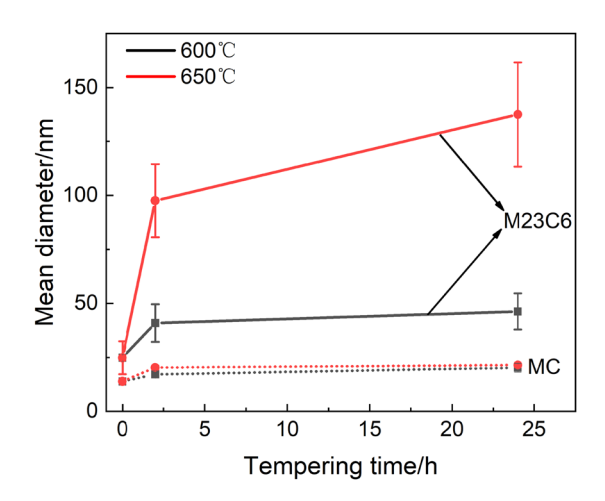


Figure 11: Evolution of main carbide size for 5CrNiMoVNb steel with tempering temperature and tempering time.

is almost unchanged. After tempering at  $600^{\circ}\text{C}$  for 24 h, the average diameter of  $M_{23}\text{C}_6$  carbides is coarsened from 24.84 to 46.31 nm and the coarsening rate is relatively low. When the tempering temperature increases to 650°C, the average diameter of  $M_{23}\text{C}_6$  carbides is coarsened to 137.44 nm. The estimated coarsening rate coefficient of  $M_{23}\text{C}_6$  at a temperature of 650°C is about 30 times as much as that at a temperature of 600°C, which is slightly higher than the calculated result. Overall, the precipitation strengthening effect of fine carbides is high and the recovery and recrystallization of the martensite matrix can be suppressed to some extent, for the relatively low coarsening rate of carbides in the 5CrNiMoVNb steel, which is probably

the mechanism that the 5CrNiMoV steel possesses excellent thermal stability.

## **4 Conclusions**

The hardness reduction of the novel hot-work die steel 5CrNiMoVNb at 600 and 650°C is 35 and 45% lower than that of the 5CrNiMoV steel, respectively. The thermal stability and tempering softening resistance of the 5CrNiMoVNb steel are significantly better.

The initial microstructure of the 5CrNiMoVNb steel consists of lath martensite and fine secondary carbides evenly dispersed on the martensite. After being tempered at 600°C and 650°C, the carbides are slightly coarsened and the martensite matrix undergoes recovery and recrystallization, which is the main reason for the decrease of thermal stability.

Due to the reasonable design of the medium and strong carbide-forming elements, the carbides in the 5CrNiMoVNb steel are mainly MC and  $M_{23}C_6$  with low coarsening coefficients, and the content of these two carbides is almost constant below 670°C. The fine MC and  $M_{23}C_6$  carbides show strong pinning and dragging effects of fine carbides on the dislocations and suppress martensite recovery and recrystallization to a certain extent, which is the thermal stability mechanism of the novel hot-work die steel 5CrNiMoVNb.

**Acknowledgments:** The authors gratefully acknowledge financial support from the Natural Science Foundation of

Sugian City (K202137), Sugian Key Laboratory of High Performance Composite Materials (M202109) and Multifunctional material research and development platform of Suqian University (2021pt04).

Funding information: This work was financially supported by Natural Science Foundation of Suqian City (K202137).

**Author contributions:** Z.Q.H. designed the experiments, performed the data analysis, and prepared the manuscript. K.K.W. performed the material thermodynamic calculations and revised the manuscript.

Conflict of interest: The authors state no conflict of interest.

Data availability statement: The raw data required to reproduce these findings are available to download from https://data.mendeley.com/drafts/gjy48nwb58.

## References

- Markezic, R., I. Naglic, N. Mole, and R. Sturm. Experimental and numerical analysis of failures on a die insert for high pressure die casting. Engineering Failure Analysis, Vol. 95, 2019, pp. 171-180.
- Gronostajski, Z., M. Kaszuba, S. Polak, M. Zwierzchowski, A. Niechajowicz, and M. Hawryluk. The failure mechanisms of hot forging dies. Materials Science and Engineering A, Vol. 657, 2016, pp. 147-160.
- Cheng, X., S. Qianqian, and J. Wu. High temperature wear characteristics of a new hot work die steel CH95. Journal of Wuhan University of Technology - Materials Science Edition, Vol. 21, No. 3, 2006, pp. 7-11.
- [4] Lu, X., Y. F. Zhou, X. L. Xing, Q. A. Tai, H. Guan, L. Y. Shao, et al. Failure analysis of hot extrusion die based on dimensional metrology, micro-characterization and numerical simulation -A case study of Ti alloy parts. Engineering Failure Analysis, Vol. 73, 2017, pp. 113-128.
- Garg, A. and A. Bhattacharya. Strength and failure analysis of similar and dissimilar friction stir spot welds: Influence of different tools and pin geometries. Material and Design, Vol. 127, 2017, pp. 272-286.
- Cong, D., H. Zhou, Z. Ren, H. Zhang, L. Ren, C. Meng, et al. Thermal fatigue resistance of hot work die steel repaired by partial laser surface remelting and alloying process. Optics and Lasers In Engineering, Vol. 54, No. SI, 2014, pp. 55-61.
- Moreira, A. B., R. O. Sousa, P. Lacerda, L. M. M. Ribeiro, A. M. P. Pinto, and M. F. Vieira. Microstructural characterization of TiC-white cast-iron composites fabricated by in situ technique. Materials, Vol. 13, No. 1, 2020, id. 209.
- Li, Y. and X. Wang. Microstructure evolution of a simulated coarse-grained heat-affected zone of T23 steel during aging. Metallurgical and Materials Transactions A: Physical

- Metallurgy and Materials Science, Vol. 51, No. 3, 2020, pp. 1183-1194.
- [9] Chu, D.-J., H.-Y. Kim, J. Lee, and W.-S. Jung. Investigation of precipitation sequence during creep in 2.25Cr-1Mo steel. Materials Characterization, Vol. 164, 2020, id. 110328.
- [10] Yu, X.-S., C. Wu, R.-X. Shi, and Y.-S. Yuan. Microstructural evolution and mechanical properties of 55NiCrMoV7 hot-work die steel during quenching and tempering treatments. Advances in Manufacturing, Vol. 9, No. 4, 2021, pp. 520-537.
- [11] Xiang, S., R. Wu, W. Li, T. Hu, and S. Huang. Improved red hardness and toughness of hot work die steel through tungsten alloying. Journal of Materials Engineering and Performance, Vol. 30, No. 8, 2021, pp. 6146-6159.
- [12] Xia, S. W., P. Zuo, Y. Zeng, and X. Wu. Influence of nickel on secondary hardening of a modified AISI H13 hot work die steel. Materialwissenschaft und Werkstofftechnik, Vol. 50, No. 2, 2019, pp. 197-203.
- [13] Ning, A., W. Mao, X. Chen, H. Guo, and J. Guo. Precipitation behavior of carbides in H13 hot work die steel and its strengthening during tempering. Metals-Basel, Vol. 7, No. 3, 2017, id. 70.
- [14] Li, J., J. Li, L. Wang, and L. Li. Study on carbide in forged and annealed H13 hot work die steel. High Temperature Materials and Processes, Vol. 34, No. 6, 2015, pp. 593-598.
- Wieczerzak, K., P. Bala, R. Dziurka, T. Tokarski, G. Cios, T. Koziel, et al. The effect of temperature on the evolution of eutectic carbides and M7C3  $\rightarrow$  M23C6 carbides reaction in the rapidly solidified Fe-Cr-C alloy. Journal of Alloys and Compounds, Vol. 698, 2017, pp. 673-684.
- [16] He, M. Y., Y. F. Shen, N. Jia, and P. K. Liaw. C and N doping in highentropy alloys: A pathway to achieve desired strength-ductility synergy. Applied Materials Today, Vol. 25, 2021, id. 101162.
- [17] He, M., N. Jia, X. Liu, Y. Shen, and L. Zuo. Abnormal chemical composition fluctuations in multi-principal-element alloys induced by simple cyclic deformation. Journal of Materials Science & Technology, Vol. 113, 2021, pp. 287-295.
- [18] He, L. Z., Q. Zheng, X. F. Sun, G.C. Hou, H. R. Guan, and Z. Q. Hu. M23C6 precipitation behavior in a Ni-base superalloy M963. Journal of Materials Science, Vol. 40, No. 11, 2005, pp. 2959-2964.
- [19] He, L. Z., Q. Zheng, X. F. Sun, H. R. Guan, Z. Q. Hu, A. K. Tieu, et al. Effect of carbides on the creep properties of a Ni-base superalloy M963. Materials Science and Engineering, Vol. 397, No. 1-2, 2005, pp. 297-304.
- [20] Zhang, Z., X. Sun, Z. Wang, Z. Li, Q. Yong, and G. Wang. Carbide precipitation in austenite of Nb-Mo-bearing lowcarbon steel during stress relaxation. Materials Letters, Vol. 159, 2015, pp. 249-252.
- [21] Yang, R. C., K. Chen, H. X. Feng, and H. Wang. Determination and Application of Larson-Miller Parameter for Heat Resistant Steel 12Cr1MoV and 15CrMo. Acta Metallurgica Sinica (English Letters), Vol. 17, No. 4, 2009, pp. 471-476.
- [22] Springer, P. and U. Prahl. Pinning effect of strain induced Nb (C,N) on case hardening steel under warm forging conditions. Journal of Materials Processing Technology, Vol. 253, 2018, pp. 121-133.
- [23] Mondiere, A., V. Deneux, N. Binot, and D. Delagnes. Controlling the MC and M2C carbide precipitation in Ferrium (R) M54 (R) steel to achieve optimum ultimate tensile strength/fracture toughness balance. Materials Characterization, Vol. 140, 2018, pp. 103-112.